New sugar-based gelators bearing a *p*-nitrophenyl chromophore: remarkably large influence of a sugar structure on the gelation ability

Natsuki Amanokura,[a] Kenji Yoza,[a] Hideyuki Shinmori,[b] Seiji Shinkai *[ab] and David N. Reinhoudt [c]

[a] *Chemotransfiguration Project, Japan Science and Technology Corporation, Aikawa, Kurume, Fukuoka 839-0861, Japan*
[b] *Department of Chemistry and Biochemistry, Graduate School of Engineering, Kyushu University, Hakozaki, Higashi-ku, Fukuoka 812-8581, Japan*
[c] *Chemotransfiguration Project, Faculty of Chemical Technology, University of Twente, 7500 AE Enschede, The Netherlands*

Received (in Cambridge) 8th September 1998, Accepted 9th October 1998

Three sugar-integrated gelators bearing a *p*-nitrophenyl group as a chromophore were synthesised. D-Mannose-based compound **3** was too soluble in most organic solvents to act as a gelator whereas D-galactose-based compound **2** was sparingly soluble in most organic solvents. D-Glucose-based compound **1** was moderately soluble and acted as an excellent gelator, gelating 10 solvents tested. The possible correlation between the gelation ability and the gelator structure is discussed on the basis of the intermolecular hydrogen-bonding interactions detectable by FT-IR spectroscopy. CD spectral measurements showed that the *p*-nitrophenyl groups in the gel fibrils of **1** are stacked in the clockwise direction [*i.e.*, with (*R*)-helicity]. SEM observation of the xerogels showed that in most cases the gelator forms a three-dimensional network with 30–100 nm frizzled fibrils. Only when they were prepared from the methylcyclohexane solution, was the helical structure (although in part) observed.

Introduction

The development of new gelators of organic solvents has recently attracted much attention from many chemists. They not only gelate various organic solvents but also create novel fibrous superstructures which can be characterised by SEM observation of the xerogels.[1–12] The gelators can be classified into two categories according to the difference in the driving force for the molecular aggregation: *viz*. hydrogen bond-based gelators and nonhydrogen-bond-based gelators. Typical examples of the former category are aliphatic amide derivatives,[1–4] whereas examples of the latter category are cholesterol derivatives[6–9,12] and anthracene derivatives.[10] The superstructures of the organic gels prepared from aliphatic amide derivatives showed that they satisfy the complementarity of the intermolecular hydrogen-bonding interactions using hydrogen-bond-donor–hydrogen-bond-acceptor couples.[5–9,13] This observation stimulated us to use saccharides as a hydrogen-bond-forming segment in the gelators, because one can easily introduce a variety of hydrogen-bond-forming, chiral segments into gelators by appropriate selection from a saccharides library. In the literature, examples of saccharide-containing gelators are very limited in spite of their high potential.[8,14,15] We have now synthesised D-glucose-based **1**, D-galactose-based **2** and D-mannose-based **3** and studied their gelation abilities in detail. The *p*-nitrophenyl group was introduced as a chromophoric probe to detect the molecular orientation. Interestingly, we have found that the gelation properties are profoundly related to the saccharide structure.[16]

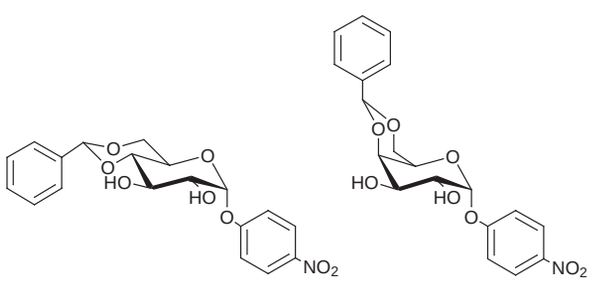

1

2

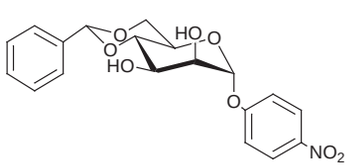

3

Results and discussion

Gelation test

Compounds **1**–**3** were synthesised by treatment of the corresponding 1-*p*-nitrophenyl derivatives with benzaldehyde in the presence of zinc chloride according to the method reported previously.[15,16] The products were identified by ^{1}H NMR and IR spectral evidence and elemental analyses (see Experimental). The gelation test was carried out for 49 solvents (Table 1). The gelator (**1**–**3**; 3.0 mg) was mixed with solvent (0.10 ml) in a septum-capped test tube and the mixture was heated until the solid was dissolved. The solution was cooled to room temperature and left for 1 h (G in Table 1 denotes that a gel was formed at this stage). Some solutions gelated at a gelator concentration below 1.0 (wt/vol)% [G(S) or super-gelator; Table 1].

It is clear from Table 1 that D-glucose-based **1** acts as an excellent gelator which can gelate 10 solvents and behaves as a super-gelator for five of those. It can generally gelate aliphatic cyclic compounds and aromatic compounds. As special

Table 1 Organic solvents tested for gelation by **1**–**3**[a]

Run	Organic solvent	Gelator 1	2	3	Run	Organic solvent	Gelator 1	2	3
1	*n*-Hexane	I	I		26	*N*,*N*-Dimethylacetamide	S	S	
2	*n*-Heptane	I	I		27	*N*,*N*-Dimethylformamide	S	S	
3	*n*-Octane	I	I	I	28	Dimethyl sulfoxide	S	S	
4	Cyclohexane	G(S)	I		29	1-Methyl-2-pyrrolidone	S	S	
5	Methylcyclohexane	G(S)	R	I	30	Acetonitrile	S	S	
6	Benzene	G	R	S	31	Methanol	R	R	S
7	Toluene	R	R		32	Ethanol	R	R	
8	*p*-Xylene	G(S)	R	R	33	*n*-Propanol	R	R	
9	Nitrobenzene	S	R	S	34	*n*-Butanol	R	R	R
10	*m*-Cresol	S	S		35	*n*-Octanol	G	R	
11	Carbon tetrachloride	G(S)	R	R	36	Benzyl alcohol	S	R	
12	Carbon disulfide	G(S)	R		37	Acetic acid	S	S	S
13	1,2-Dichloroethane	R	R		38	Hexanoic acid	R	R	
14	Dichloromethane	R	R		39	Acetic anhydride	S	S	
15	Chloroform	R	R	S	40	*n*-Propylamine	S	S	
16	Diethyl ether	G	R		41	Diethylamine	S	S	
17	Diphenyl ether	G(S)	R	S	42	Triethylamine	R	I	S
18	Tetrahydrofuran	S	S	S	43	Aniline	S	S	
19	Dioxane	S	S		44	Pyridine	S	S	
20	Ethyl formate	R	R		45	Triethylsilane	I	I	
21	Methyl acetate	R	S		46	Tetraethoxysilane	G(S)	R	
22	Ethyl acetate	S	R	S	47	2,2,2-Trifluoroethanol	S	S	
23	Ethyl malonate	S	S		48	Glycerol	R	S	
24	Acetone	S	S		49	Water	R	R	R
25	Methyl ethyl ketone	R	R	S					

[a] G = gel; G(S) = super gel; R = recrystallization; S = solution; I = insoluble.

examples, one can raise *n*-octanol and tetraethoxysilane which are also gelated. In contrast, D-galactose-based **2** generally shows a poor stability in most solvents (I = insoluble or R = recrystallized) whereas D-mannose-based **3** in more soluble in most solvents [compare S (no precipitate formed after cooling) for **3** in benzene, nitrobenzene, diphenyl ether, ethyl acetate and methanol with R for **2** in the corresponding solvents]. The foregoing results indicate that the gelation phenomena are induced by **1** which has moderate solubility, not as soluble as **3** but not as insoluble as **2**. The sole structural difference among **1**, **2** and **3** is the absolute configuration of C-2 and C-4. It is really surprising that the slight difference in the saccharide structure drastically changes the gelation ability.

Molecular motion of 1 as detected by ^{1}H NMR spectroscopy

It is expected that the molecular motion of gelators drastically changes at the sol–gel phase-transition temperature (T_{gel}). This change can be conveniently monitored by the line-broadening effect observed for the ^{1}H NMR peaks. In fact, such a phenomenon has already been reported for the related gel system.[17] We measured the ^{1}H NMR spectra of a **1** [2.0 (wt/vol)%] + benzene system at 44 ~ 86 °C. In this system, the T_{gel} was 69 °C (*vide post*). As shown in Fig. 1A, the δ_{OH} at around 2.3 ppm used as a measure shifted to lower magnetic field with the temperature drop but a discontinuous change did not appear at the T_{gel}. As shown in Fig. 1B, in contrast, the half-height peak-width ($\delta_{\frac{1}{2}}$) was nearly constant above the T_{gel} while it increased with the temperature drop below the T_{gel}. The results imply that the sol–gel phase-transition influences the mobility of the gelator as detected by the $\delta_{\frac{1}{2}}$ but is not so effective as to influence the strength of the hydrogen-bonding interaction as detected by the δ_{OH}.

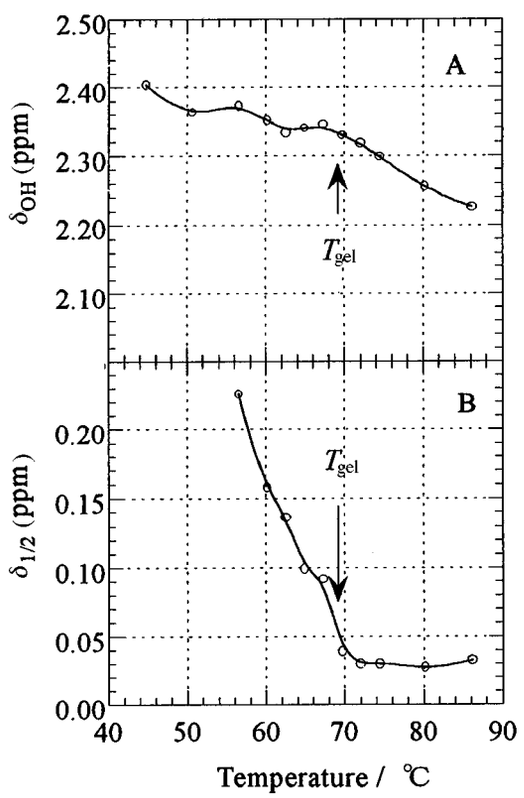

Fig. 1 Plots of (A) δ_{OH} (chemical shift of an OH group) and (B) $\delta_{\frac{1}{2}}$ (half-height peak-width of the peak) against temperature: [**1**] = 2.0 (wt/vol)%, benzene.

Intermolecular hydrogen-bonding interactions as detected by FT-IR spectroscopy

It is reasonable to assume that **1**, **2** and **3** have a different gelation ability because of a difference in the intermolecular hydrogen-bonding ability. In the FT-IR spectra of the solid samples measured as KBr disks, **1**, **2** and **3** all gave only one OH vibration peak assignable to the intermolecularly hydrogen-bonded OH groups: 3385 cm^{-1} for **1**, 3422 cm^{-1} for **2** and 3440 cm^{-1} for **3**; for **2** alone, two weak additional peaks are present at 3503 and 3559 cm^{-1}. The peak for **3** (3440 cm^{-1}) appeared at a higher frequency region than those for **1** (3385 cm^{-1}) and **2** (3422 cm^{-1}). The difference implies that in the solid state the hydrogen-bond-based intermolecular force in **3** is weaker than

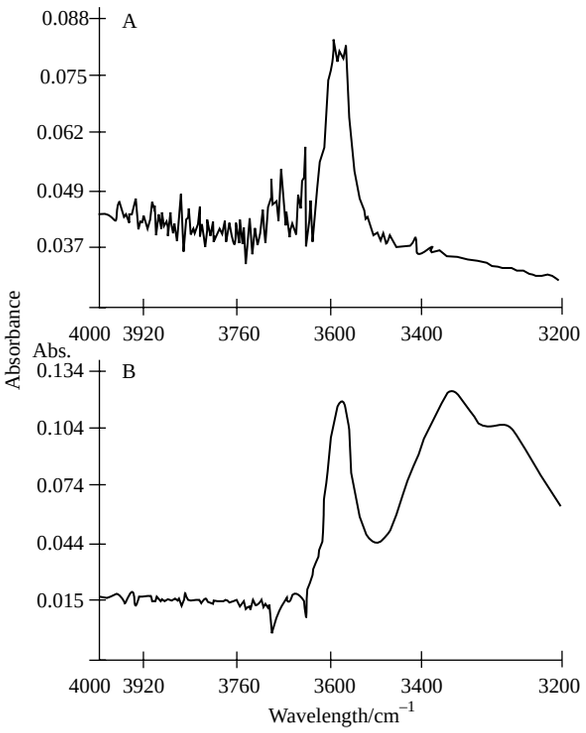

Fig. 2 FT-IR spectra of **1** [(A) 0.20 (wt/vol)% solution and (B) 1.0 (wt/vol)% gel] in benzene at 25 °C.

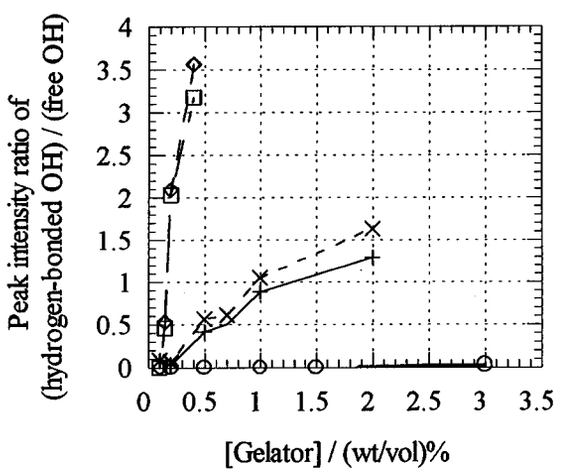

Fig. 3 Plots of the peak intensity ratio of (hydrogen-bonded ν_{OH} peak)/(free ν_{OH} peak) *vs.* the gelator concentration in benzene. ◇, ν_{OH} (3505 cm^{-1})/ν_{OH} (3571 cm^{-1}) of **2**; □, ν_{OH} (3423 cm^{-1})/ν_{OH} (3571 cm^{-1}) of **2**; ×, ν_{OH} (3385 cm^{-1})/ν_{OH} (3576 cm^{-1}) of **1**; +, ν_{OH} (3302 cm^{-1})/ν_{OH} (3576 cm^{-1}) of **1**; ○, ν_{OH} (3440 cm^{-1})/ν_{OH} (3570 cm^{-1}) of **3**.

that in **1** and **2**. A dilute benzene solution of **1** gave only one OH vibration peak for free OH groups at 3576 cm^{-1}. In contrast, the benzene gel solution gave an OH vibration peak for free OH groups at 3576 cm^{-1} and two OH vibration peaks for hydrogen-bonded OH groups at 3385 and 3302 cm^{-1}. Typical FT-IR spectra are shown in Fig. 2. As shown in Fig. 3, the hydrogen-bonded OH vibration peak was not observed for very soluble **3** up to 1.0 (wt/vol)% whereas it could be detected for sparingly soluble **2** even at 0.20 (wt/vol)%. For **1**, on the other hand, it appeared only above the sol–gel phase-transition concentration [0.40 (wt/vol)%]. It is clear, therefore, that the formation of the intermolecular hydrogen-bonds is an indispensable driving-force for gelation but the hydrogen-bonding interaction should be 'moderately strong' in order not to precipitate but to gel solvents.

Thermodynamic considerations

Previously, we derived eqn. (1) from a Schrader's relation

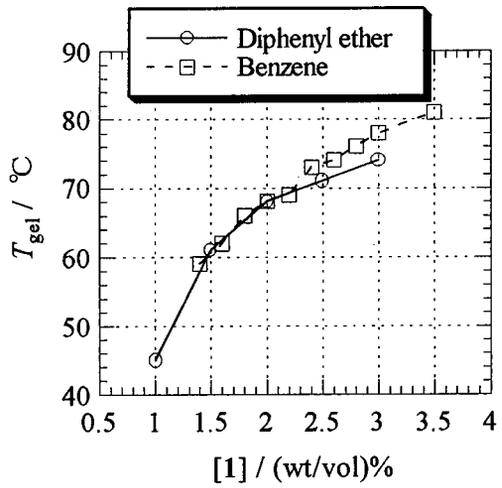

Fig. 4 Plots of T_{gel} *vs.* [**1**].

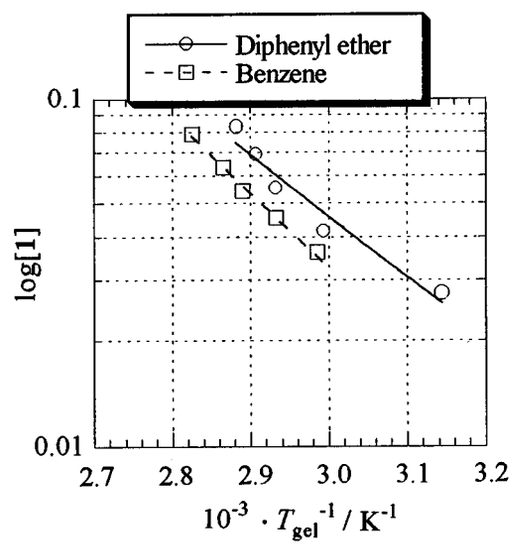

Fig. 5 Plots of log [**1**] *vs.* T_{gel}^{-1}/K^{-1}.

$$\log[\text{gelator(in mol dm}^{-3})] = -\frac{\Delta H}{2.303R} \times \frac{1}{T_{gel}} + \text{constant} \quad (1)$$

frequently used for dissolution of solid compounds into organic solvents.[7] The ΔH can be determined from the slope of a log-[gelator (in mol dm^{-3})] *vs.* T_{gel}^{-1} plot. It is known that the ΔH values are comparable with or slightly larger than ΔH_f values determined from DSC measurements at the melting point of the solid.[7] This implies that the ΔH reflects the heat capacity released at the sol–gel phase-transition temperature.

The ΔH_f values at mp determined by a DSC method were 22.1, 35.5 and 1.2 kJ mol^{-1} for **1**, **2** and **3**, respectively. Interestingly, the order of the ΔH_f values, *viz.*, **2** > **1** > **3**, correlates well with the degree of solubility (see Table 1). In particular, the ΔH_f for **3**, which is soluble in most organic solvents, is very small compared with the other two values.[18] The plots of T_{gel} *vs.* [**1**] in benzene and diphenyl ether are shown in Fig. 4. As expected, the T_{gel} rises with increasing gelator concentration. As shown in Fig. 5, plots of log [**1**] *vs.* T_{gel}^{-1} afforded straight lines with r (correlation coefficient) = 0.996 for benzene and 0.969 for diphenyl ether. The ΔH values estimated on the basis of eqn. (1) were 41 kJ mol^{-1} for benzene and 32 kJ mol^{-1} for diphenyl ether. These values are slightly larger than the ΔH_f for **1** at mp (22.1 kJ mol^{-1}). The similarity between the two enthalpy terms implies that, as discussed in detail previously,[7] the gelator fibrils have a solid-like nature and deaggregate at the sol–gel phase-transition temperature.

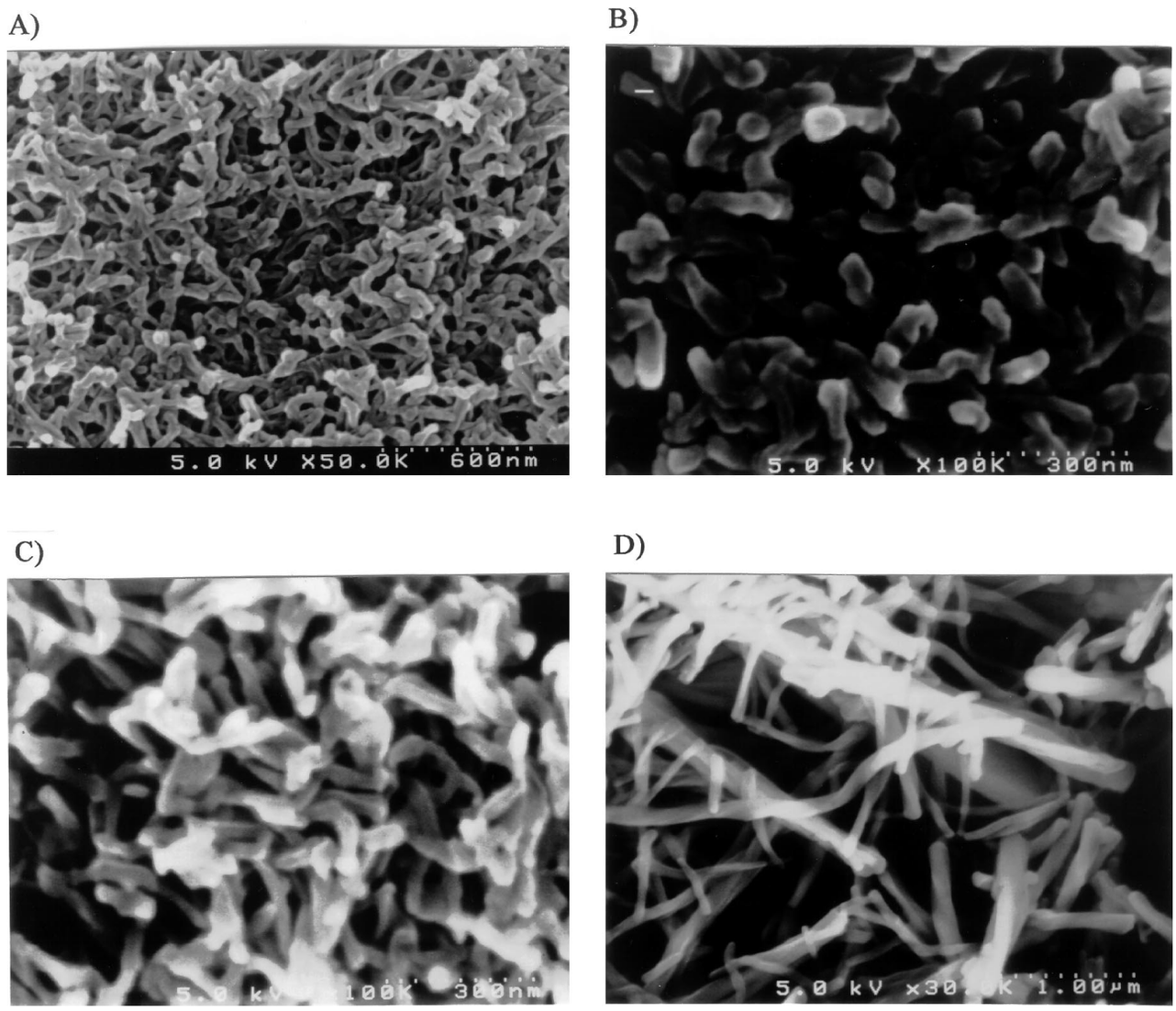

Fig. 6 SEM pictures of **1** prepared from A) benzene [3.0 (wt/vol)%], B) carbon tetrachloride [0.50 (wt/vol)%], C) cyclohexane [0.50 (wt/vol)%] and D) methylcyclohexane [0.50 (wt/vol)%] solutions.

SEM observation of xerogels

To obtain visual insights into the aggregation mode, we prepared dry samples for SEM observation.[19] We used benzene, carbon tetrachloride, cyclohexane and methylcyclohexane solutions of **1** at 0.50 ~ 3.0 (wt/vol)%. Typical SEM pictures are shown in Fig. 6. It is clear from Fig. 6 that the gelator forms a three-dimensional network with 30–100 nm frizzled fibrils. In general, the diameters of the fibrils obtained from the benzene and carbon tetrachloride solutions are smaller than the diameters of those obtained from the cyclohexane and methylcyclohexane solutions. The fibrils obtained from the methylcyclohexane solution (Fig. 6D) partly contain the helical structure. Careful observation shows that it is all left-handed helix. Although it is not yet clear why such a higher-order structure is created only in methylcyclohexane, it is intriguing to see if the macroscopic chirality observed by SEM is reflected by the microscopic chirality as detected by circular dichroism (CD) spectroscopy.

Chirality of the aggregates as detected by CD spectroscopy

Since **1** has a chromophoric *p*-nitrophenyl group, the higher-order chirality of the aggregates may be detected by CD spectroscopy. In the absorption spectra, the λ_{max} of **1** in benzene appeared at 295 nm in the sol phase and at 284 nm at the gel phase. The slight but significant blue shift in the gel phase suggests that the *p*-nitrophenyl groups are assembled according to the H-type aggregation mode.[20] As shown in Fig. 7B, the CD spectra of **1** [0.10 (wt/vol)%] were scarcely changed at 10 ~ 60 °C in the sol phase. On the other hand, a significant spectral change appeared at 1.0 (wt/vol)%: the sol–gel phase-transition occurred at 45 °C and the CD maximum (287 nm at 60 °C) in the sol phase (>45 °C) shifted to longer wavelength (296 nm) in the gel phase (<45 °C).[21]

Provided that these CD spectra result from an overlap of dissolved **1** and aggregated **1**, the "true" CD spectra for aggregated **1** would be expressed as the difference spectra obtained by subtracting Fig. 7A from Fig. 7B at each temperature. Since the concentration in Fig. 7A is 10 times higher than that in Fig. 7B whereas the cell width in Fig. 7A is 0.1 times shorter than that in Fig. 7B, one can directly compare these two figures. The difference spectra thus obtained are shown in Fig. 8. It is clearly seen from Fig. 8 that the exciton-coupling-type CD band is observable only for the gel phase. The $\theta = 0$ wavelength (288 nm) shows a good agreement with the absorption maximum in the gel phase (284 nm). The CD sign with the first positive Cotton effect and the second negative Cotton effect implies that the *p*-nitrophenyl groups are stacked in the clockwise direction [*i.e.*, with (*R*)-chirality]. The results mean that the D-glucose moieties are packed into the fibrils by hydrogen-bonding interactions and the *p*-nitrophenyl moieties are forced to orientate into (*R*)-chirality.

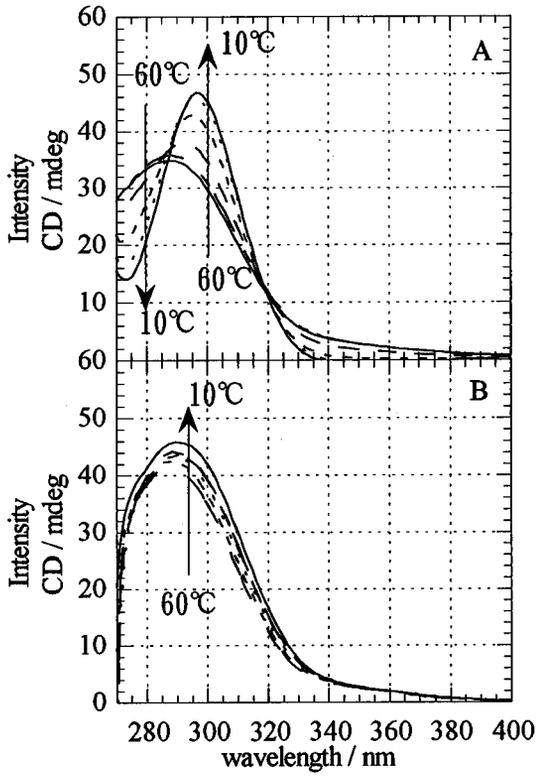

Fig. 7 CD spectra of **1** in benzene at (A) 0.10 (wt/vol)% in 1.0 mm cell width and (B) 1.0 (wt/vol)% in 0.1 mm cell width: the temperatures are 10, 20, 30, 40, 50 and 60 °C.

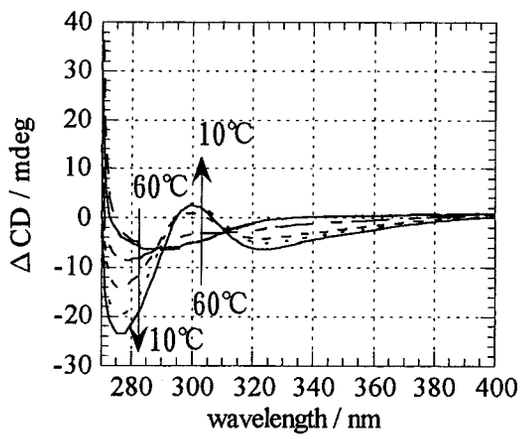

Fig. 8 Difference CD spectra obtained by subtracting Fig. 7B from Fig. 7A.

Computational considerations

In order to obtain some rationale for the differences in solubility or in gelation ability, we executed computational studies using MM3 and MOPAC. Fig. 9 shows the energy-minimized structures of C1-**1**, C1-**2** and C1-**3** starting from the C1 structure of the pyranose form by MM3: the minimized energies are 196, 130 and 167 kJ mol^{-1}, respectively. It is seen from Fig. 9 that all the gelators feature a bent conformation between the pyranose ring and the *p*-nitrophenyl ring. This is due to the C-1 configuration in which the *p*-nitrophenyl group occupies the axial position. Here, one controversial problem comes to mind: in the stereochemistry of cyclohexane derivatives the bulky substituent tends to occupy the *equatorial* position. This stereochemical requirement should also be valid in the pyranose ring. This is achieved by ring inversion of the C1 structure to the 1C structure. In **1** and **3**, both 4-OR and 5-CH_2OR occupy the *equatorial* position, so that inversion to the 1C structure enforces them to take the *trans-axial* positions. This is impossible because 4-OR and 5-CH_2OR form a 1,3-dioxane ring. In other words, the C1 structure in Fig. 9 is the only possible conformation for **1** and **3**. In contrast, 4-OR and 5-CH_2OR in **2** occupy the *axial* and *equatorial* positions, respectively. Hence, it is possible for the pyranose ring in **2** to invert into the 1C structure: in this conformation the *p*-nitrophenyl group can shift to the less crowded equatorial position. Thus, we tried to find the most stable structure by MM3 starting from the 1C structure. We thus obtained 1C-**2** as an energy-minimized structure (minimized energy 150 kJ mol^{-1}: Fig. 9).

As shown in Fig. 9, C1-**1** and C1-**3** adopt an L-shaped, folded conformation whereas 1C-**2** is more or less flat. Undoubtedly, flat 1C-**2** should be more favourable to molecular stacking.[7] Conceivably, this is the primary reason why **2** shows poor solubility in most organic solvents. In addition, *axial* 2-OH and 3-OH in 1C-**2** should be efficiently utilized for the formation of intermolecular hydrogen-bonds. Actually, this was found in the ν_{OH} bands in FT-IR spectroscopy (Fig. 3). The heat of formation values calculated by MOPAC PM3 were estimated to be −773, −769, −786 and −777 kJ mol^{-1} for C1-**1**, C1-**2**, C1-**3** and 1C-**2**, respectively. Although the clear difference in stability between C1-**2** and 1C-**2** could not be found by the computational studies, we believe that the advantage brought from the intermolecular hydrogen-bonding interaction should stabilize the 1C-**2** structure.

Conclusion

The present study has demonstrated that saccharides are promising building-blocks for new gelators with different gelation abilities and different three-dimensional network structures. Surprising is the finding that the gelation ability is remarkably changed by a slight change in the saccharide configuration. It was shown, however, that the gelation ability is predictable to some extent by the physical parameters such as ν_{OH} in FT-IR, δ_{OH} in ^{1}H NMR and ΔH_f in DSC: these parameters always appear in the order **2** (too cohesive) > **1** (moderately cohesive: suited to gelation) > **3** (less cohesive: too soluble). We believe that convenience in the synthesis and diversity of the products cannot be attained in a more simple fashion than with saccharides as building-blocks. The present paper has shown the high potential of saccharide-based gelators.

Experimental

p-Nitrophenyl 4,6-*O*-benzylidene-*α*-D-glucopyranoside (1)

Compound **1** was synthesised according to the method in the literature.[15] A mixture of benzaldehyde (1.0 ml, 9.9 mmol) and *p*-nitrophenyl *α*-D-glucopyranoside (500 mg, 1.66 mmol) was stirred with zinc chloride (240 mg, 1.77 mmol) under a nitrogen atmosphere. The reaction was continued at room temperature for 20 h. After the reaction mixture was added to water (15 ml), the product thus precipitated was collected by filtration. This product on the filter paper was washed with water and hexane and then reprecipitated by THF–hexane; yield 300 mg, 46% (calculated from *p*-nitrophenyl *α*-D-glucopyranoside), mp 158–159 °C; ^{1}H NMR (DMSO-d_6) δ 3.54–4.06 and 5.47–5.56 [m, 8H, sugar-CH (H-2 ~ H-6) and OH], 5.62 (s, 1H, PhCH), 5.82 (d, 1H, sugar H-1), 7.30–7.43 (m, 7H, ArH in Ph and *p*-nitrophenyl-*o*-H), 8.25 (d, 2H, *p*-nitrophenyl-*m*-H); IR (KBr) 3670–3000 (ν_{OH}), 1340 and 1510 (ν_{N-O}), 1060 (ν_{C-O-C}) cm^{-1}. Found: C, 58.29; H, 4.87; N, 3.56. Calc. for $C_{19}H_{19}O_8N$: C, 58.61; H, 4.92; N, 3.60%.

p-Nitrophenyl 4,6-*O*-benzylidene-*α*-D-galactopyranoside (2)

Compound **2** was synthesised according to a method similar to that used for **1**; yield 640 mg, 99% (calculated from *p*-nitrophenyl *α*-D-galactopyranoside), mp 191–192 °C; ^{1}H NMR (DMSO-d_6) δ 3.69–4.24 and 5.06–5.25 [m, 8H, sugar-CH

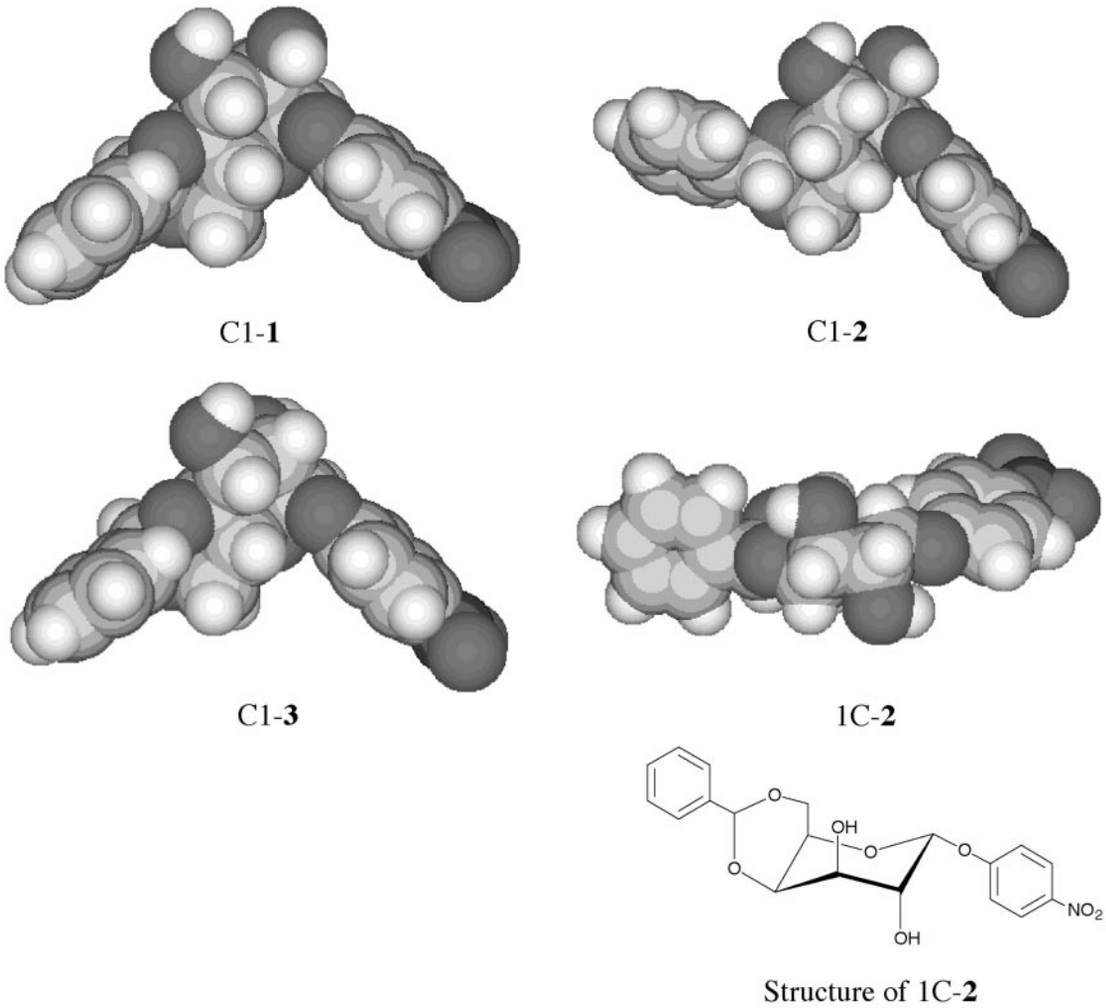

Fig. 9 Energy-minimized structures of **1**, **2** and **3** predicted from MM3: only **2** can adopt both the C1 and 1C structures.

(H-2 ~ H-6) and OH], 5.59 (s, 1H, PhCH), 5.85 (d, 1H, sugar H-1), 7.31 (d, 2H, *p*-nitrophenyl-*o*-H), 7.37–7.48 (m, 5H, ArH in Ph), 8.24 (d, 2H, *p*-nitrophenyl-*m*-H); IR (KBr) 3660–3100 (ν_{OH}), 1330 and 1500 (ν_{N-O}), 1070 (ν_{C-O-C}) cm^{-1}. Found: C, 58.35; H, 4.91; N, 3.58. Calc. for $C_{19}H_{19}O_8N$: C, 58.61; H, 4.92; N, 3.60%).

p-Nitrophenyl 4,6-*O*-benzylidene-*α*-D-mannopyranoside (3)

Compound **3** was synthesised according to a method similar to that used for **1**; and was purified by column chromatography (silica gel, $CHCl_3$–MeOH = 10 : 1; $R_f = 0.1$). The product obtained was reprecipitated by THF–hexane; yield 27 mg, 4% (calculated from *p*-nitrophenyl *α*-D-mannopyranoside), mp 103–104 °C; ^{1}H NMR ($CDCl_3$) δ 3.01 (d, 2H, OH), 3.85–4.32 [m, 6H, sugar-CH (H-2 ~ H-6)], 5.62 (s, 1H, PhCH), 5.72 (s, 1H, sugar H-1), 7.17 (d, 2H, *p*-nitrophenyl-*o*-H), 7.39–7.52 (m, 5H, ArH in Ph), 8.27 (d, 2H, *p*-nitrophenyl-*m*-H); IR (KBr) 3680–3100 (ν_{OH}), 1344 and 1516 (ν_{N-O}), 1096 (ν_{C-O-C}) cm^{-1}. Found: C, 56.10; H, 5.21; N, 3.34%. Calc. for $C_{19}H_{19}O_8N$: C, 58.61; H, 4.92; N, 3.60% ($C_{19}H_{19}O_8N \cdot 0.9H_2O$: C, 56.27; H, 5.17; N, 3.45%).[22]

Solvent effects on gelation

The gelators and the solvents were put in a septum-capped sample tube and heated until the solid was dissolved. The solution was cooled at room temperature for 1 h. If the stable gel was observed, it was classified as G [it was classified as G(S) if the concentration of gelator was under 1.0 (wt/vol)%].

Gel–sol phase-transition temperatures

The test tube containing the gel was immersed upside down in a thermostatted water bath or oil bath. The temperature was raised at a rate of 2 °C min^{-1}. Here, the T_{gel} is defined as the temperature at which the gel disappears.

SEM measurements

A Hitachi S-900S scanning electron microscope was used for taking the SEM pictures. A thin gel was prepared in a sample tube and frozen in liquid nitrogen. The frozen specimen was evaporated by a vacuum pump for 3–5 h. The dry sample thus obtained was shielded by gold. The accelerating voltage of SEM was 5 kV and the emission current was 10 μA.

CD and LD measurements

1 [0.01 ~ 1.0 (wt/vol)%] was mixed with benzene or methylcyclohexane in a septum-capped sample tube and the mixture was heated until **1** was dissolved. Before it was gelated, the solution was put into an optical cell. The mixture in the cell was reheated and cooled to form the gel. Then, the measurement was started. CD and LD spectra were measured using a water-jacket cell (0.1, 1.0 and 10 mm optical pass length). The temperature was controlled by a water flow passing through the cell directly.

Apparatus for spectral measurements

^{1}H NMR spectra were measured on a Bruker ARX 300

apparatus. IR spectra were obtained in NaCl cells using a Shimazu FT-IR 8100 spectrometer. UV spectra were measured on a JASCO V-570 spectrophotometer. CD and LD spectra were measured on a JASCO J-720 spectrometer.

Computational methods

Energy-minimization of **1**–**3** was carried out by MM3 using AccuModel 1.0 (Microsimulation L.A. Systems Inc.) on a Macintosh computer and by MOPAC PM3 using CS Chem-office Chem 3D (CambridgeSoft Corporation) on an NEC computer.

References

1 (*a*) K. Hanabusa, K. Okui, K. Karaki and H. Shirai, *J. Chem. Soc.*, *Chem. Commun.*, 1992, 1371 and references cited therein; (*b*) K. Hanabusa, Y. Yamada, M. Kimura and H. Shirai, *Angew. Chem.*, *Int. Ed. Engl.*, 1996, **35**, 1949; (*c*) K. Hanabusa, K. Shimura, K. Hirose, M. Kimura and H. Shirai, *Chem. Lett.*, 1996, 885; (*d*) K. Hanabusa, A. Kawakami, M. Kimura and H. Shirai, *Chem. Lett,*, 1997, 191.

2 E. J. De Vries and R. M. Kellogg, *J. Chem. Soc.*, *Chem. Commun.*, 1993, 238.

3 M. Takafuji, H. Ihara, C. Hirayama, H. Hachisako and K. Yamada, *Liq. Cryst.*, 1995, **18**, 97.

4 J.-E. S. Sobna and F. Fages, *Chem. Commun.*, 1997, 327.

5 E. Otsumi, P. Kamasas and R. G. Weiss, *Angew. Chem.*, *Int. Ed. Engl.*, 1996, **35**, 1324 and references cited therein.

6 P. Terech, I. Furman and R. G. Weiss, *J. Phys. Chem.*, 1995, **99**, 9558 and references cited therein.

7 K. Murata, M. Aoki, T. Suzuki, T. Hanada, H. Kawabata, T. Komori, F. Ohseto, K. Ueda and S. Shinkai, *J. Am. Chem. Soc.*, 1994, **116**, 6664 and references cited therein.

8 T. D. James, K. Murata, T. Harada, K. Ueda and S. Shinkai, *Chem. Lett.*, 1994, 273.

9 (*a*) S. W. Jeong, K. Murata and S. Shinkai, *Supramol. Sci.*, 1996, **3**, 83; (*b*) S. W. Jeong and S. Shinkai, *Nanotechnology*, 1997, **8**, 179.

10 T. Brotin, R. Utermöhlen, F. Fagles, H. Bouas-Laurebt and J.-P. Desvergne, *J. Chem. Soc.*, *Chem. Commun.*, 1991, 416.

11 J. van Esch, S. De Feyter, R. M. Kellogg, F. De Schryver and B. L. Feringa, *Chem. Eur. J.*, 1997, **3**, 1238.

12 For recent comprehensive reviews see: (*a*) P. Terech and R. G. Weiss, *Chem. Rev.*, 1997, **97**, 3133; (*b*) S. Shinkai and K. Murata, *J. Mater. Chem.*, 1998, **8**, 485.

13 It is considered, however, that the hydrogen-bond complementarity in the gel network is more disordered than that in the crystal.[9]

14 S. Yamasaki and H. Tsutsumi, *Bull. Chem. Soc. Jpn.*, 1996, **69**, 561 and references cited therein.

15 M. Svaan and T. Anthonsen, *Acta Chem. Scand.*, *Ser. B*, 1986, **40**, 119.

16 K. Yoza, Y. Ono, K. Yoshihara, T. Akao, H. Shinmori, M. Takeuchi, S. Shinkai and D. N. Reinhoudt, *Chem. Commun.*, 1998, 907.

17 M. Aoki, K. Nakashima, H. Kawabata, S. Tsutsui and S. Shinkai, *J. Chem. Soc.*, *Perkin Trans. 2*, 1993, 347.

18 Compounds **1** and **2** were isolated as dehydrated samples whereas it was very difficult to obtain a dehydrated sample from **3.** This may also be related to the high solubility and the small ΔH_f value.

19 For the preparation of dry samples for SEM observation see refs. 7 and 9.

20 T. Kunitake, *Angew. Chem.*, *Int. Ed. Engl.*, 1992, **31**, 709 and references cited therein.

21 We measured the LD spectra in the gel phase under identical measurement conditions and confirmed that their contribution was negligible relative to that of the CD spectra.

Paper 8/07001F